Platelet-Derived Growth Factor BB Enhances Osteogenesis of Adipose-Derived But Not Bone Marrow-Derived Mesenchymal Stromal/Stem Cells

BEN P. HUNG,[a,b] DAPHNE L. HUTTON,[a,b] KRISTEN L. KOZIELSKI,[a,b] COREY J. BISHOP,[a,b]
BILAL NAVED,[c] JORDAN J. GREEN,[a,b] ARNOLD I. CAPLAN,[d] JEFFREY M. GIMBLE,[e]
AMIR H. DORAFSHAR,[f] WARREN L. GRAYSON[a,b,g]

Key Words. Tissue engineering • Platelet-derived growth factor • Bone • Stem cells

[a]Department of Biomedical Engineering and [b]Translational Tissue Engineering Center, The Johns Hopkins University School of Medicine, Baltimore, Maryland, USA; [c]Fischell Department of Biomedical Engineering, University of Maryland, College Park, Maryland, USA; [d]Department of Biology, Case Western Reserve University, Cleveland, Ohio, USA; [e]Department of Medicine and Surgery, Tulane University, New Orleans, Louisiana, USA; [f]Department of Plastic Surgery, The Johns Hopkins Hospital, Baltimore, Maryland, USA; [g]Department of Materials Science & Engineering, The Johns Hopkins University Whiting School of Engineering, Baltimore, Maryland, USA

Correspondence: Warren L. Grayson, Ph.D., 400 N. Broadway, Smith 5023, Baltimore, Maryland 21231, USA. Telephone: 410-502-6306; Fax: 410-502-6308; e-mail: wgrayson@jhmi.edu

ABSTRACT

Tissue engineering using mesenchymal stem cells (MSCs) holds great promise for regenerating critically sized bone defects. While the bone marrow-derived MSC is the most widely studied stromal/stem cell type for this application, its rarity within bone marrow and painful isolation procedure have motivated investigation of alternative cell sources. Adipose-derived stromal/stem cells (ASCs) are more abundant and more easily procured; furthermore, they also possess robust osteogenic potency. While these two cell types are widely considered very similar, there is a growing appreciation of possible innate differences in their biology and response to growth factors. In particular, reports indicate that their osteogenic response to platelet-derived growth factor BB (PDGF-BB) is markedly different: MSCs responded negatively or not at all to PDGF-BB while ASCs exhibited enhanced mineralization in response to physiological concentrations of PDGF-BB. In this study, we directly tested whether a fundamental difference existed between the osteogenic responses of MSCs and ASCs to PDGF-BB. MSCs and ASCs cultured under identical osteogenic conditions responded disparately to 20 ng/ml of PDGF-BB: MSCs exhibited no difference in mineralization while ASCs produced more calcium per cell. siRNA-mediated knockdown of PDGFRβ within ASCs abolished their ability to respond to PDGF-BB. Gene expression was also different; MSCs generally downregulated and ASCs generally upregulated osteogenic genes in response to PDGF-BB. ASCs transduced to produce PDGF-BB resulted in more regenerated bone within a critically sized murine calvarial defect compared to control ASCs, indicating PDGF-BB used specifically in conjunction with ASCs might enhance tissue engineering approaches for bone regeneration. STEM CELLS 2015;33:2773–2784

SIGNIFICANCE STATEMENT

The findings of this study demonstrate that adipose-derived stem cells (ASCs) exhibit a fundamentally different osteogenic response to platelet-derived growth factor (PDGF) signaling from bone marrow-derived mesenchymal stem cells (MSCs). In the presence of physiological concentrations of PDGF-BB (20 ng/ml), ASCs increase the expression of osteogenic genes and, in the presence of a phosphate source, significantly upregulate mineral deposition. MSCs do not show a corresponding increase in either mineral deposition or gene expression. This finding suggests that while the two cell types exhibit significant similarities, they may possess intrinsically different biochemistries.

INTRODUCTION

It is estimated that more than 1 million bone fractures requiring hard tissue transplantation occur annually in the U.S., incurring an economic burden of $3 billion per year [1]. The demand for donor tissue greatly outstrips the supply of both allogeneic and autologous sources, underscoring the pressing need for alternative approaches to reconstruct bone. In recent years, tissue engineering (TE) has emerged as a promising method for producing bone grafts de novo. In the traditional TE paradigm, cells are housed inside biomaterial scaffolds and signaled with bioactive factors [2]; the scaffold provides mechanical and structural support while the bioactive factors guide the cells in regenerating tissue.

For bone regeneration specifically, the marrow-derived mesenchymal stem cell (MSC) is the most widely studied cell type. MSCs, isolated from bone marrow aspirate, have the ability to differentiate into the three classic mesenchymal lineages of bone, fat, and

cartilage [3]; furthermore, their immunomodulatory characteristics suggest their potential in allogeneic transplantation [4]. The study of MSC-based therapies for bone regeneration has reached clinical trials for applications in, but not limited to, osteonecrosis [5], nonunion repair [6], and spinal fusion [7]. MSCs, however, are a fairly rare population within bone marrow, comprising less than 0.01% of the nucleated population. To address this shortcoming, recent studies have investigated the presence of similar cells in other tissues of the body, most notably within fat. These adipose-derived stromal/stem cells (ASCs) also have the capability to differentiate down the classic mesenchymal lineages and represent a larger population within adipose tissue, accounting for up to approximately 5% of nucleated cells in the collagenase-released stromal vascular fraction (SVF) [8, 9]. While it is generally recognized that MSCs and ASCs exhibit similar surface immunophenotypes and multilineage differentiation characteristics, recent studies have called into question the extent of their similarities [10].

In particular, studies into the osteoinductive potential of platelet-derived growth factor BB (PDGF-BB), prompted by the observation of heightened PDGF-BB levels within bone fracture microenvironments [11, 12], have largely determined that PDGF-BB is not osteoinductive when signaling MSCs. In fact, PDGF-BB was shown to inhibit mineralization [13–16] and when the beta receptor for PDGF, PDGFRβ, was deleted using Cre-LoxP recombination, mineralization of MSCs was restored even in the presence of PDGF-BB [17]. In contrast, our group has recently shown a dose-dependent increase in calcification per cell in ASCs when signaled with PDGF-BB [18]. More recent studies have exploited this, using ASCs in fibrin matrices incorporating PDGF-BB [19]; however, to date, no direct comparison of MSCs and ASCs in their osteogenic response to PDGF-BB has been performed to resolve the apparent contradiction.

A potential difference between MSCs and ASCs is of high importance in the use of TE approaches to treat bone defects. PDGF-BB is a known mitogen [20] and chemoattractant [21] and it has been observed that injection of PDGF-BB into fracture sites accelerates bone healing [22]. Given the in vitro observations that PDGF-BB does not directly promote osteogenesis in MSCs, it is thought that PDGF-BB in this case is largely acting through recruitment of endogenous repair cells. The notion that PDGF-BB can directly enhance ASC mineralization, however, presents the possibility that the use of ASCs in conjunction with PDGF-BB for bone repair can more efficiently make use of both the cellular and biomolecular components.

In this study, we hypothesize that the osteogenic response of MSCs and ASCs to PDGF-BB is different at a fundamental genetic level. To test this hypothesis, the objectives of this study are (a) to investigate the differences in osteogenic response of MSCs and ASCs at a cellular and genetic level, (b) to use siRNA-mediated knockdown of PDGFRβ for loss-of-function evidence that specifically PDGF-BB leads to enhanced mineralization of ASCs but not of MSCs, and (c) to demonstrate the application of this finding using ASCs overexpressing PDGFB in an in vivo murine calvarial defect model.

MATERIALS AND METHODS

Isolation and Source of Cells

All tissues obtained for this study were obtained under Institutional Review Board approved protocols with patient con-

sent. To ensure the observed phenomena are cell-type specific rather than donor-dependent, the initial characterization study was performed using three donors for MSCs, denoted M1, M2, and M3; and three donors for ASCs, denoted A1, A2, and A3. Donor M1 (late 20s, male) was commercially obtained from Lonza (Basel, Switzerland), while Donors M2 (32-year-old male) and M3 (27-year-old male) were isolated at Case Western Reserve University following established marrow isolation procedures [23–25]. Briefly, aspirated iliac crest bone marrow was mixed with culture medium and centrifuged to remove adipocytes. MSCs were isolated from the resulting cell pellet via centrifugation in a Percoll gradient and the MSC-enriched fraction was plated. Donors A1 (54-year-old female) and A2 (50-year-old female) were isolated from lipoaspirate using established protocols [26, 27] at Johns Hopkins Medical Institutions, while Donor A3 (47-year-old female) was isolated at Tulane University School of Medicine. Briefly, harvested lipoaspirate tissue was digested in 1 mg/ml collagenase type I (Worthington Biochemical Corporation, Lakewood, NJ) for 1 hour at 37°C. The released cells were then centrifuged to obtain the SVF pellet; the pellet was then resuspended and plated to obtain passage 0 ASCs. Cells from all six donors were characterized via flow cytometry for surface expression of CD31, CD34, CD73, CD90, and PDGFRβ as previously described [27]. In this study, PDGFRβ was studied specifically as it preferentially binds PDGF-BB.

Culture Conditions

For all experiments, cells were expanded for use at passage 2. Expansion medium consisted of Dulbecco's modified Eagle medium (DMEM) with 4.5 g/l glucose (Life Technologies, Frederick, MD) supplemented with 10% (vol/vol) fetal bovine serum (FBS; Atlanta Biologicals, Flowery Branch, GA), 100 U/ml penicillin and 100 µg/ml streptomycin (Cellgro, Manassas, VA), and 1 ng/ml basic fibroblast growth factor (PeproTech, Rocky Hill, NJ). Subsequent to expansion, cells were cultured in one of four conditions: namely, the control (−), control (+), osteogenic (−), and osteogenic (+) conditions. The control (−) medium consisted of DMEM with 1 g/l glucose, 100 U/ml penicillin and 100 µg/ml streptomycin, and 6% (vol/vol) FBS. Control (+) medium consisted of control (−) medium with the addition of 20 ng/ml recombinant human PDGF-BB (PeproTech), a concentration determined based on our previous work [18]. The osteogenic (−) medium consisted of control (−) medium with 10 mM β-glycerophosphate (Sigma Aldrich, St. Louis, MO) and 50 µM ascorbic acid (Sigma Aldrich). Finally, osteogenic (+) medium consisted of osteogenic (−) medium with 20 ng/ml PDGF-BB. For all conditions, PDGF-BB was replenished twice a week. These culture conditions were established from our previous studies [18]. Unless otherwise noted, all osteogenic cultures were carried out for 3 weeks.

Characterization of Mineralization Response to PDGF-BB

MSCs and ASCs were cultured under control (−), control (+), osteogenic (−), and osteogenic (+) conditions for 3 weeks and then subjected to Alizarin Red S (Sigma Aldrich) or von Kossa (silver nitrate and sodium thiosulfate both from Sigma Aldrich) staining for qualitative assessments. Quantitatively, samples were subject to the Quant-It PicoGreen dsDNA assay

(Invitrogen, Carlsbad, CA) and the Stanbio LiquiColor calcium assay (Stanbio, Boerne, TX) to determine calcium content normalized to cell number. DNA content was converted to cell number using 6.24 pg/MSC and 7.23 pg/ASC, determined by performing the DNA assay on known numbers of the cells specifically used in this study (data not shown).

Real-Time Polymerase Chain Reaction

To investigate the genetic expression of MSCs and ASCs under the four conditions, real-time polymerase chain reaction (RT-PCR) was performed at 1, 2, and 3 weeks of culture for β-Actin (BA), Runx2, osteocalcin (OCN), osteonectin (OSN), and collagen I (Col-I). Cells were digested using TRIzol reagent (Life Technologies) and the mRNA isolated with chloroform washes. The mRNA was further purified and concentrated using isopropanol and ethanol washes and used to produce cDNA using the iScript cDNA Synthesis Kit (Bio-Rad Laboratories, Hercules, CA). cDNA was then subject to RT-PCR using custom-designed primers. The primer sequences for all primers used in this study can be found in Table 1. For all analysis, the delta-delta Ct method was used in which the housekeeping gene (BA) and the appropriate (−) group were subtracted from all other Ct readings.

Monomer Synthesis

Bioreducible monomer 2,2'-disulfanediylbis(ethane-2,1-diyl) (BR6) was synthesized as previously described [28, 29]. Briefly, bis(2-hydroxyethyl) disulfide (10 mmol) was acrylated with acryloyl chloride (300 mmol) in the presence of triethylamine (TEA; 300 mmol) in anyhydrous tetrahydrofuran (THF) for 24 hours. TEA HCl precipitate was removed via filtration, and THF was removed via rotary evaporation. The product was further purified by dissolving it in dichloromethane (DCM) and washing five times with a 0.2 M solution of Na_2CO_3 and three times with water. The organic phase was dried with Na_2SO_4 and DCM was removed via rotary evaporation. BR6 structure and purity were verified by ^{1}H NMR [28].

Polymer Synthesis

To obtain loss-of-function evidence, siRNA against PDGFRβ was delivered to MSCs and ASCs using bioreducible poly(β-amino ester) (PBAE)-based nanoparticles. Bioreducible PBAEs were synthesized in a method similar to Kozielski et al. [28]. Base monomer BR6 was polymerized with side chain monomer 4-amino-1-butanol (S4) at a ratio of 1.05:1 at 500 mg/ml in anhydrous tehtrahydrofuran (THF) at 60°C for 24 hours while stirring. Polymers were endcapped at a concentration of 100 mg/ml in THF with either 2-(3-(aminopropyl)amino)methanol (E6) or 1-(3-aminopropyl)−4-methylpiperazine (E7) at 0.2 M for 1 hour at room temperature while stirring. Polymers were precipitated in diethyl ether to remove unreacted monomer and THF. The precipitate was recovered by centrifugation and solvent decanting. The polymer was washed and isolated a second time, and residual ether was removed under vacuum for 48 hours. The resulting polymers BR6-S4-E6 (R646) and BR6-S4-E7 (R647) were stored in dimethyl sulfoxide at 100 mg/ml at −20°C.

Nanoparticle Screen Using Green Fluorescent Protein

Two polymers, R646 and R647, were used to deliver siRNA against green fluorescent protein (siGFP) to MSCs transduced

Table 1. Primer sequences used for real-time polymerase chain reaction

Gene name		Primer sequence (5'–3')
β-Actin	Fwd.	AGTTGCGTTACACCCTTTCTTG
	Rev.	TCACCTTCACCGTTCCAGTTT
RUNX-2	Fwd.	GTCTCACTGCCTCTCACTTG
	Rev.	CACACATCTCCTCCCTTCTG
OCN	Fwd.	GTGACGAGTTGGCTGACC
	Rev.	TGGAGAGGAGCAGAACTGG
OSN	Fwd.	TCGGCATCAAGCAGAAGGATA
	Rev.	CCAGGCAGAACAACAAACCAT
Col-1	Fwd.	GAGAGGAAGGAAAGCGAGGAG
	Rev.	GGGACCAGCAACACCATCT
PDGF-B	Fwd.	GTTGAGGTGGCTGTAGATGGT
	Rev.	AGGGTGGAGGTAGAGAGATGAA
PDGFR-β	Fwd.	TGAGGCTTTGGAGGAATC
	Rev.	CCTTGCTTCATCTGGACA

with GFP by lentivirus, a procedure we have used previously to screen nanoparticles [30]. Briefly, lentiviral production was produced using 293T cells and the ViraSafe Lentiviral Packaging System (Cell Biolabs, San Diego, CA). MSCs were seeded at 6,000 cells per square centimeter, allowed to adhere for 1 day, and given virus at 8×10^7 viral particles per milliliter for 4 hours (an approximate multiplicity of infection of 80) under serum-free conditions. Expansion medium was added after the viral incubation step and transduction was allowed to continue for 72 more hours, after which medium was changed to clean expansion medium and the cells were allowed to proliferate to confluence. The efficiency of transduction was approximately 86% as determined by fluorescence-activated cell sorting [30].

GFP$^+$ MSCs were screened for polymeric siRNA delivery using Ambion *Silencer* siRNA targeting GFP (siGFP) with sequence 5'-CAAGCUGACCCUGAAGUUCUU (sense) and 3'-GAA CUUCAGGGUCAGCUUGCC (antisense), or Ambion *Silencer* Negative Control #1 siRNA (scrRNA) with sequence 5'-AGUAC UGCUUACGAUACGGTT (sense) and 3'-CCGUAUCGUAAGCAG UACUTT (antisense) (Life Technologies). Nanoparticles were formed by dissolving siRNA and polymers separately in 25 mM sodium acetate (NaAc), mixing the siRNA and polymer solutions, and allowing nanoparticles to self-assemble for 10 minutes. The cell culture medium was removed and replaced with 100 μl of serum-free medium, then 20 μl of nanoparticle solutions was added directly to the cell culture media. Polymers R646 and R647 were used at final concentrations of 360, 270, or 180 μg/ml, and siRNA were at final concentrations of 80, 40, or 20 nM. Following a 2-hour incubation with cells, the nanoparticle-containing media were removed and replaced with fresh, complete cell culture medium.

At 24 hours post-transfection, viability was assessed using a Cell Titer 96 AQueous One MTS Cell Proliferation assay (Promega, Madison, WI) following manufacturer's instructions. Absorbance at 490 nm was read using a BioTek Synergy 2 Microplate Reader and viability of cells in treated wells was calculated by normalizing to absorbance values of cells in untreated wells.

GFP knockdown was measured every day for 3.5 weeks using a BioTek Synergy 2 Microplate Reader by reading the total fluorescence of each well at 485 ± 10 nm excitation and 520 ± 10 nm emission. In previous work, we have found that this method of measuring GFP expression correlates well with

data acquired via flow cytometry [30] while enabling facile tracking of GFP knockdown over time. Fluorescence values from wells treated with siRNA were normalized to values from wells treated with scrRNA and subtracted from 1 to determine knockdown.

Knockdown of PDGFRβ

siRNA against PDGFRβ (siPDGFRβ) was delivered to both MSCs and ASCs using the transfection protocol above. At 1, 2, and 3 weeks, knockdown of PDGFRβ was quantified using both RT-PCR of PDGFRβ and flow cytometry via an antibody against the receptor (Santa Cruz, Santa Cruz, CA).

Separately, siPDGFRβ was delivered to MSCs and ASCs and cells were cultured under control (−), osteogenic (−), and osteogenic (+) conditions for 3 weeks. After the culture period, calcium and DNA content were quantified as outlined above.

Murine Critically Sized Calvarial Defect Model

For the final portion of the study, two different cell groups were created by lentiviral transduction: (a) ASCs transduced with PDGFB (DNASU plasmid HsCD00437330 [31]) and (b) ASCs transduced with the fluorescent protein mCherry (plasmid kindly provided by Don Zack's laboratory). Transduction was performed following the protocol above and PDGFB-transduced ASCs were verified by RT-PCR and enzyme-linked immunosorbent assay (ELISA, PeproTech). In addition, cells were cultured under control (−) and osteogenic (−) conditions for 3 weeks and then subject to DNA and calcium assays as outlined above to determine whether the overexpressed PDGF-BB was having a mitogenic and mineralization effect.

For the in vivo study, ASCs were encapsulated at 2×10^7 cells per milliliter in fibrin gels containing final concentrations of 8 mg/ml fibrinogen and 2 U/ml thrombin. Cells in fibrin were seeded into porous polycaprolactone scaffolds (diameter: 4 mm, height: 644 μm, porosity 60% by volume) mixed with mineralized particles printed with a custom three-dimensional printer [32]. This geometry was chosen to match the geometry of the murine calvarial defect described below. In addition, a third group was produced with the same scaffolds and fibrin, but containing no cells. For seeding, cells were suspended in fibrinogen and thrombin was added at the proper ratio. Prior to gelation, the mixture was pipetted into the pore spaces of the scaffold and subsequent gelation held the cells in place within the pore spaces.

Eight 8-week-old male FOXN1-knockout mice (Jackson Laboratories, Bar Harbor, ME) were operated on, resulting in 16 sites with $n = 4$ for ASCs overexpressing PDGFB, $n = 4$ for ASCs transduced with mCherry, $n = 4$ for acellular controls, and $n = 4$ unoperated controls. In all cases, IACUC-approved procedures were followed. For creation of the defect, previously established methods were adapted [33, 34]. Briefly, a 4-mm circular knife (Medicon, Tuttlingen, Germany) was used to excise 4-mm pieces of calvaria, with special care made to avoid damaging the underlying dura mater. The location of the defect was kept consistent from animal to animal by placement between the coronal and lambdoid sutures and approximately 1 mm lateral to the sagittal suture.

Mice were imaged using computerized tomography (CT) at 8 weeks postimplantation, sacrificed, and calvariae were excised for histological analysis. Imaging was performed on a Gamma Medica X-SPECT small animal system (Gamma Medica, Salem, NH) with 80 kV peak voltage and 600 μA current. Reconstruction was performed with voxel size 100 μm and threshold 15,300/65,535. For sectioning, samples were fixed in 3.7% formalin overnight and fixed samples were infiltrated with 30% sucrose, frozen in Tissue Tek OCT medium, and cut into 10 μm-thick sections. Cryosections were mounted and dried on Superfrost Plus slides, followed by rehydration in water before staining with von Kossa/van Gieson, Hematoxylin and Eosin (H&E; Sigma), or immunohistochemistry. Immunohistochemistry was performed by blocking for 30 minutes (10% normal serum/0.2% Triton X), followed by overnight incubation with primary antibody (0.5 μg/ml mouse anti-human Lamin A/C; Abcam, Cambridge, Britain) at 4°C, 1 hour incubation with Cy3-conjugated donkey anti-mouse (Jackson ImmunoResearch, West Grove, PA) at room temperature, and nuclear counterstain for 4′-6-diamidino-2-phenylindole (DAPI; Sigma). Cryosections were imaged using an inverted Zeiss Axio Observer microscope.

Statistics

Unless otherwise noted, statistical comparisons used the two-tailed Student's t test at α level 0.05.

RESULTS

Cell Characterization

Surface marker characterization matched well-documented profiles for MSCs/ASCs: all cells were negative for CD31, the MSCs negative for CD34, the ASCs weakly positive for CD34, and all cells were positive for both CD73 and CD90 (Supporting Information Fig. S1, bottom).

Osteogenic Response of MSCs and ASCs to PDGF-BB

After 3 weeks of culture, MSCs and ASCs were stained with Alizarin Red S and von Kossa for a qualitative assessment of mineralization. MSCs and ASCs stained negatively under both control (−) and control (+) conditions (Fig. 1A–1H), as no calcium phosphate source was present in these conditions. Under osteogenic (−) conditions, both cell types stained positively for mineralization (Fig. 1I–1L); the ASC group stained more intensely positive under osteogenic (+) conditions (Fig. 1O, 1P). MSCs under osteogenic (+) conditions stained with similar intensity to MSCs under osteogenic (−) conditions (Fig. 1M, 1N). Because PDGF-BB is a mitogen, we considered the possibility that the more intense staining with ASCs was simply due to the presence of more cells. To address this, calcium content was quantified and normalized to cell counts. ASCs under osteogenic (+) conditions displayed significantly higher calcium per cell than did ASCs under osteogenic (−) conditions, an observation that did not hold for MSCs; there was no difference in calcium per cell between MSCs under osteogenic (−) conditions versus MSCs under osteogenic (+) conditions (Fig. 1, bottom). In particular, this held for cells across all donors examined. Also of note, in all cases PDGF-BB acted as a mitogen, with osteogenic (+) groups displaying higher cell counts at the end of 3 weeks compared to cells under osteogenic (−) conditions; this held regardless of cell type and donor (Supporting Information Fig. S1, top),
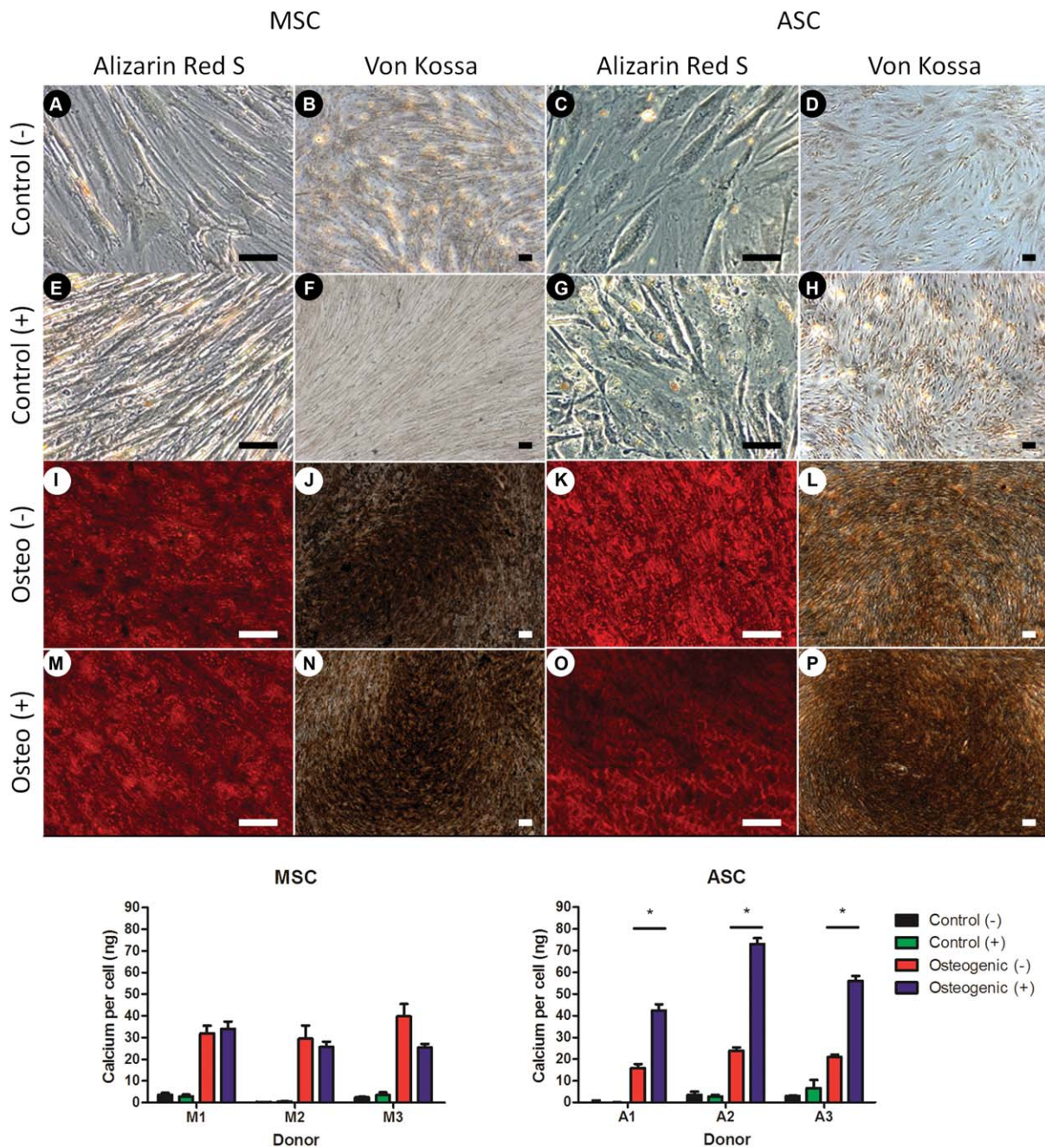
Figure 1. MSC and ASC mineralization under the effect of exogenous platelet-derived growth factor BB (PDGF-BB). MSCs and ASCs were cultured under control (−), control (+), osteogenic (−), and osteogenic (+) conditions for 3 weeks. Staining after 3 weeks of culture revealed no mineralization under either control condition **(A–H)** and an enhancement of mineralization under the presence of PDGF-BB in ASCs **(O, P** vs. **K, L)** but not in MSCs **(M, N** vs. **I, J)**. Quantitative calcium per cell analysis revealed the increased mineralization was on a per-cell basis and the ASC-specific phenomenon was a donor-independent effect over six donors (bottom). Scale bar = 100 μm. *, $p < .05$. Abbreviations: ASC, adipose-derived stromal/stem cells; MSC, mesenchymal stem cell.

confirming that the MSCs were able to respond to the PDGF-BB, just not in an osteogenic manner.

To determine whether there was a genetic mechanism underlying this data, RT-PCR was performed at 1, 2, and 3 weeks of culture. Cells cultured under control (+) conditions, despite being unable to form mineral, displayed a genetic response: MSCs generally downregulated osteogenic genes compared to MSCs under control (−) conditions, whereas ASCs generally upregulated those genes (Fig. 2, left). With the addi-

tion of osteogenic factors, the same trend held, with ASC expression of the same genes upregulated under osteogenic (+) conditions compared to expression levels under osteogenic (−) conditions and the opposite true for MSCs (Fig. 2, right).

Loss-of-Function Effect on MSC and ASC Osteogenic Response to PDGF-BB

The polymer screen indicated that both R646 and R647 were able to knockdown GFP, with R646 slightly outperforming
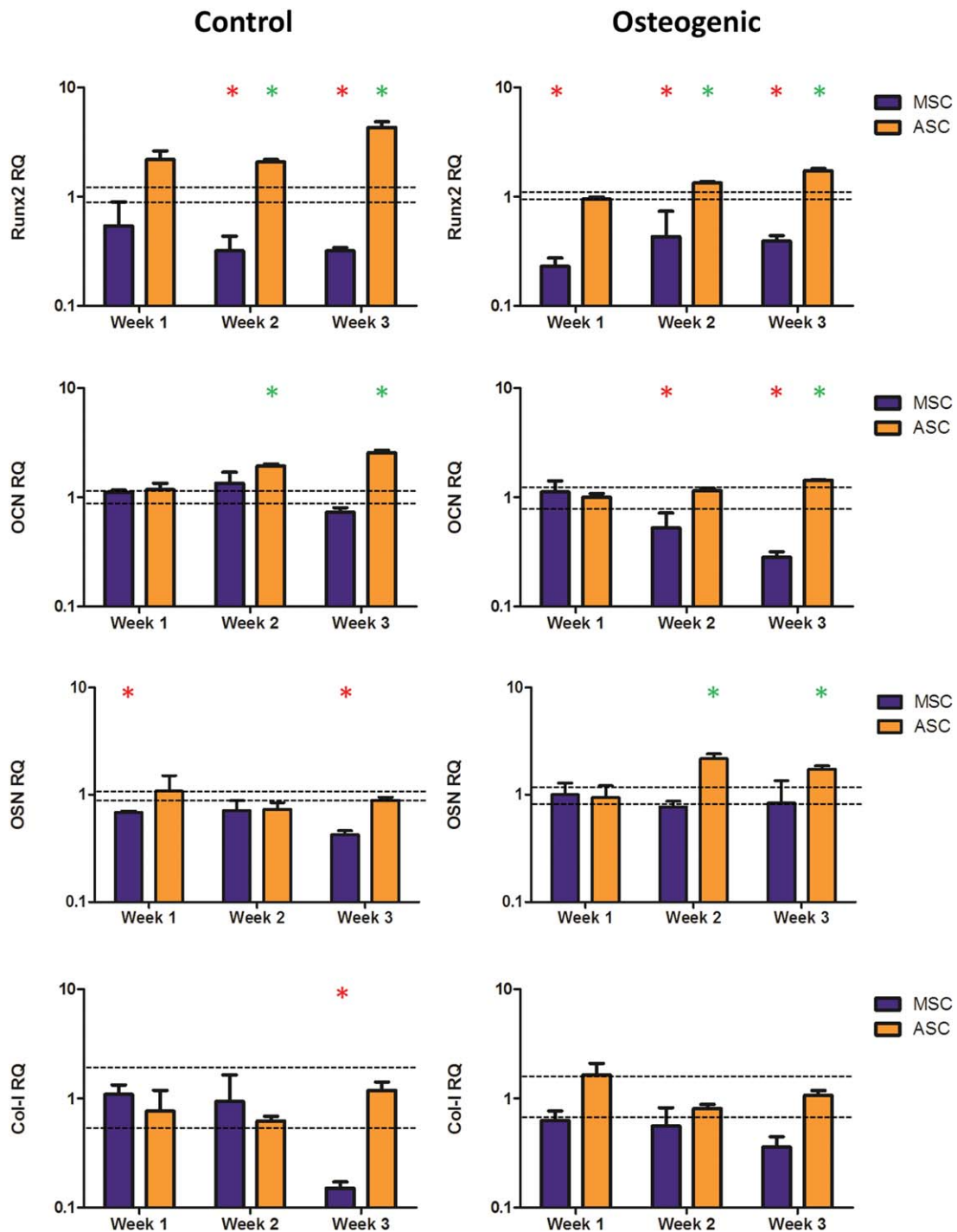
Figure 2. Gene expression of MSCs and ASCs under the effect of exogenous platelet-derived growth factor BB (PDGF-BB). Gene expression analysis of the osteogenic genes Runx2, osteocalcin, osteonectin, and collagen-I via real-time polymerase chain reaction showed that exogenous PDGF-BB under control (+) conditions tended to downregulate genes in MSCs while upregulating them in ASCs (left; normalized to expression under control medium conditions without PDGF-BB, variation shown by dotted lines). The same observations held when considering osteogenic conditions (right; normalized to expression under osteogenic medium conditions without PDGF-BB, variation shown by dotted lines). All expression quantities are relative to β-actin as housekeeping gene. Red asterisk denotes downregulation compared to ($-$) conditions while green asterisk denotes upregulation compared to ($-$) conditions, $p < .05$. Abbreviations: ASC, adipose-derived stromal/stem cells; MSC, mesenchymal stem cell; OCN, osteocalcin; OSN, osteonectin.

R647. Increasing siRNA concentration up to 40 nM enhanced knockdown, while increasing polymer concentration beyond 180 μg/ml either had no effect on or actually reduced the extent of knockdown. Both polymers displayed similar cyto-

toxicity levels at 24 hours post-transfection. Based on these results (Supporting Information Fig. S2), polymer R646 at 180 μg/ml and siRNA concentration of 40 nM was selected for subsequent studies.
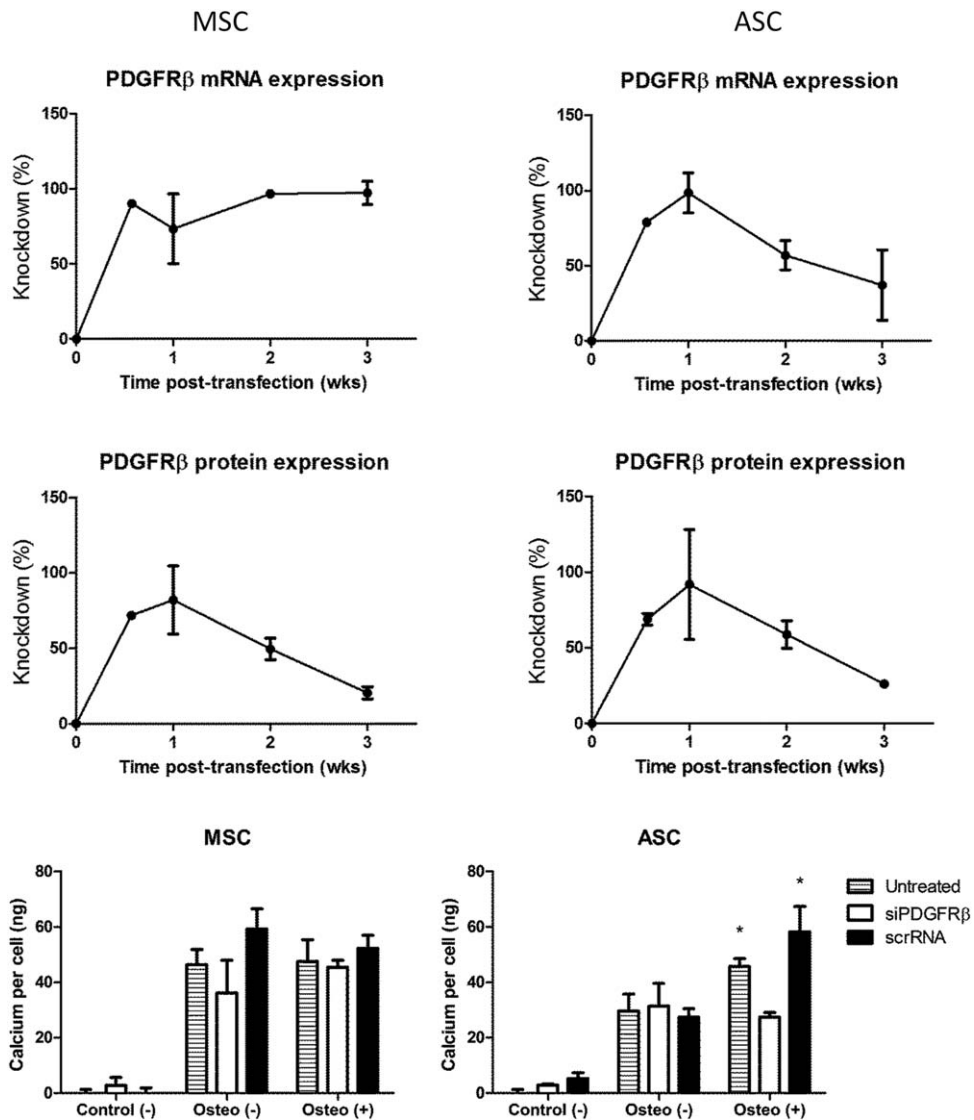
Figure 3. Loss-of-function experiment for the effect of exogenous platelet-derived growth factor BB (PDGF-BB). siRNA against the receptor PDGFRβ was delivered to MSCs and ASCs using a reducible poly(β-amino ester) vehicle. Knockdown of receptor relative to a scrambled control was evident for more than 3 weeks via both real-time polymerase chain reaction and antibody-based flow cytometry (top). While MSC mineralization at 3 weeks post-transfection was unaffected irrespective of treatment or the presence of PDGF-BB, silenced ASCs lost the enhancement of mineralization under osteogenic (+) conditions in contrast to untreated ASCs or ASCs given the scrambled control. *, $p < .05$ compared to corresponding osteogenic (−) quantities via two-way ANOVA. Abbreviations: ASC, adipose-derived stromal/stem cells; MSC, mesenchymal stem cell.

R646 knocked down PDGFRβ well, achieving a peak knock-down approaching 100% at 1 week post-transfection and declining afterward to ∼30% at 3 weeks post-transfection (Fig. 3, top). After 3 weeks of culture under control (−), osteogenic (−), and osteogenic (+) conditions (the control [+] group was omitted in this experiment since no mineralization occurred in the absence of osteogenic medium), cells were subjected to calcium per cell quantification to determine the effect of knocking down the receptor. MSCs produced similar levels of calcium per cell irrespective of the presence of PDGF-BB or whether cells were treated with siRNA, reinforcing the notion that PDGF-BB did not directly affect MSC mineralization (Fig. 3, bottom). In contrast, while the silenced ASCs showed no statistically significant difference between osteogenic (−) and osteogenic (+) groups, untreated ASCs

and ASCs given scrRNA retained a statistically higher calcium per cell reading in the osteogenic (+) groups as compared to the osteogenic (−) groups via a two-way ANOVA with $p < .05$ (Fig. 3, bottom) despite the knockdown being less pronounced in ASCs at the mRNA level at later time points. This loss-of-function data further supports the observations that ASCs upregulate calcium production on a per-cell basis when signaled with PDGF-BB, whereas MSCs do not.

Transduction of PDGFB into ASCs and Effect on Murine Calvarial Defect

Both RT-PCR and PDGF-BB ELISA confirmed the efficacy of transduction, with the PDGFB mRNA and protein greatly upregulated compared to cells transduced with mCherry by
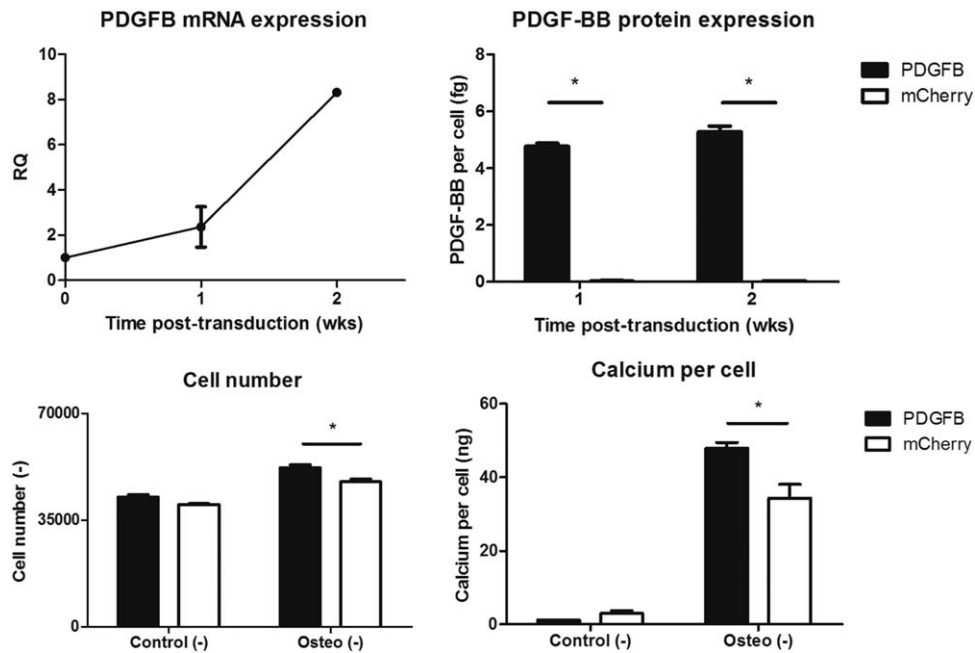
Figure 4. Verification of lentiviral transduction. Lentivirus containing the gene PDGFB or mCherry was used to transduce adipose-derived stromal/stem cells (ASCs). PDGFB-transduced ASCs overexpressed the gene and produced more protein compared to mCherry-transduced controls as determined by real-time polymerase chain reaction and enzyme-linked immunosorbent assay (top). The produced protein had a functional effect, increasing cell proliferation and calcium-per-cell content as evidenced by DNA and calcium assays (bottom). *, $p < .05$. Abbreviation: PDGF-BB, platelet-derived growth factor BB.
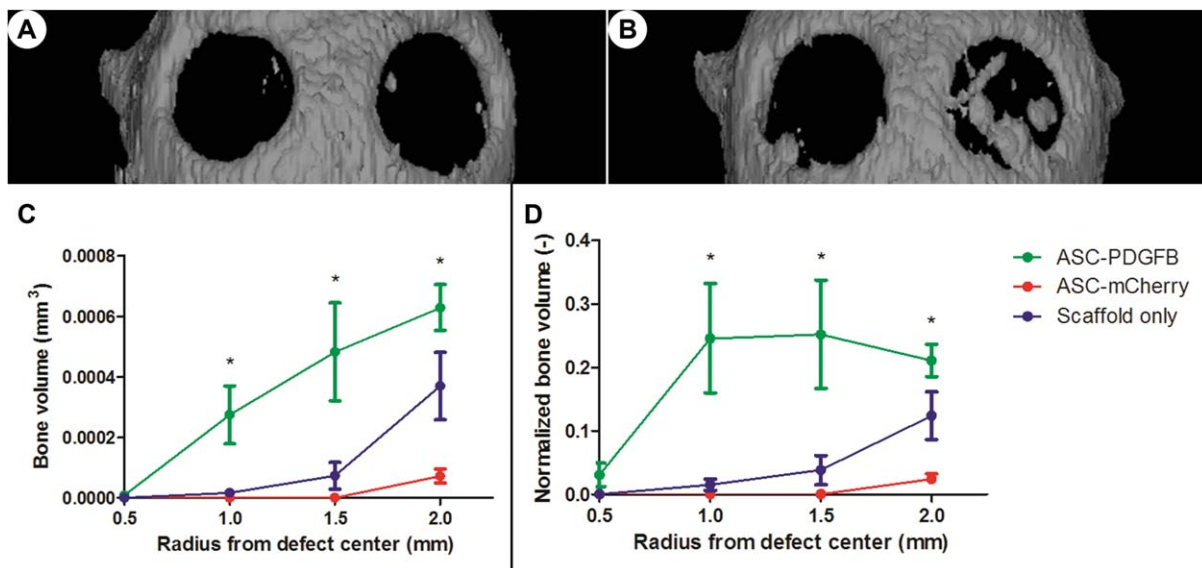
Figure 5. Computed tomography analysis of in vivo regeneration. Scaffolds seeded with mCherry-transduced ASCs (**A**, right defect), PDGFB-transduced ASCs (**B**, right defect), or empty fibrin (A, B, left defects) were implanted in critically sized 4-mm-diameter murine calvarial defects for 8 weeks. Computed tomography reconstructions (A, B) were used for quantification of bone volume within the defect. In terms of both absolute bone volume (**C**) and bone volume normalized to unoperated values (**D**), the PDGFB-transduced ASCs produced significantly more bone volume beginning at a 2-mm radius within the defect compared to both other groups. *, $p < .05$ via one-way ANOVA. Abbreviation: ASC, adipose-derived stromal/stem cells.

2 weeks post-transduction (Fig. 4, top). PDGFB-transduced cells also proliferated more under osteogenic conditions (Fig. 4, bottom left) and produced more calcium per cell (Fig. 4, bottom right) compared to mCherry-transduced cells, indicating the overexpressed PDGFB gene was having a functional effect on ASCs. PDGFB-transduced MSCs displayed similar increases in proliferation (Supporting Information Fig. S5, bottom left), but the transduction did not have an effect on MSC calcium per cell (Supporting Information Fig. S5, bottom right).
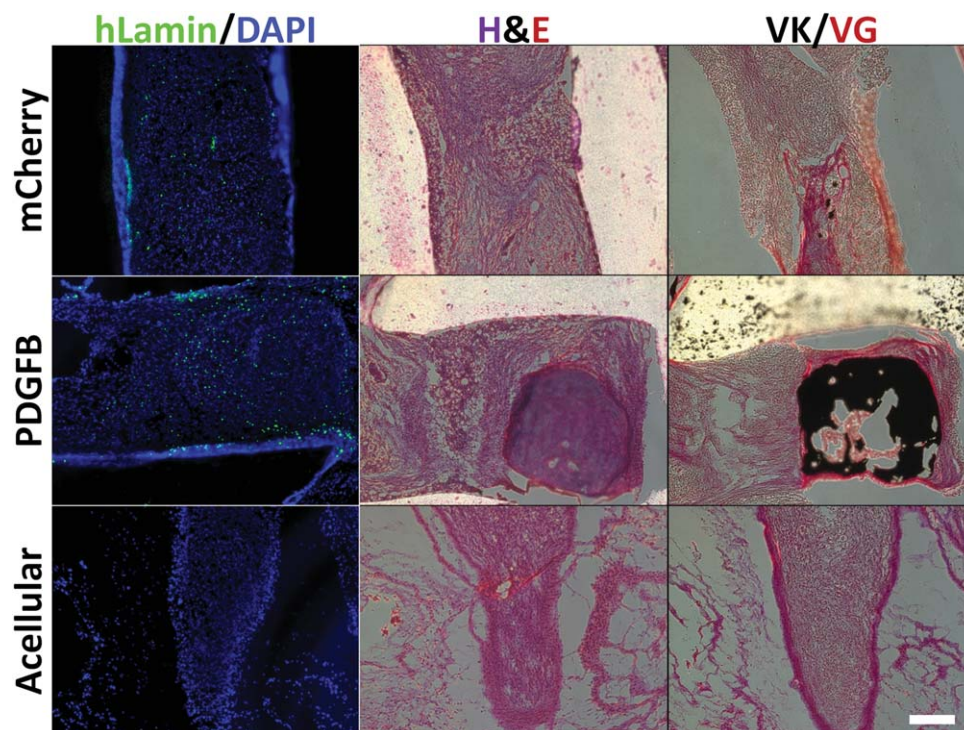
Figure 6. Histological analysis of in vivo regeneration. Eight weeks postimplantation, mice were sacrificed and scaffolds excised. Immunohistochemistry for human-specific Lamin A/C (left), hematoxylin and eosin (middle), and von Kossa/van Gieson (right) was performed to assess retention of human cells, scaffold cellularity, and bone formation, respectively. The majority of mineralization (von Kossa staining, black) occurred PDGFB-transduced group. The implanted human cells (human Lamin A/C, green) were retained within all scaffolds, with positive staining evident in all groups except for the acellular group, where no human cells were implanted. Scale bar = 200 μm. Abbreviation: DAPI, 4′-6-diamidino-2-phenylindole.

Transduced cells were encapsulated into fibrin gels and seeded into custom-printed scaffolds and implanted for 8 weeks within the murine calvarial defect. CT imaging of murine calvariae at 8 weeks postimplantation (Fig. 5A, 5B) showed a significantly higher volume of regenerated bone within the PDGFB-transduced groups compared to both other groups via one-way ANOVA both when considering absolute bone volume (Fig. 5C) or when normalizing bone volume to unoperated contralateral controls (Fig. 5D). In particular, the higher mineral content was observed throughout the scaffolds (both outer and inner regions), strongly suggesting that transplanted ASCs themselves were being signaled by the elevated PDGF-BB concentrations to undergo osteogenesis.

To investigate this further, we tested whether human ASCs remained at the defect site. Excised scaffolds were sectioned and stained with human-specific Lamin A/C with DAPI counterstain for retention of human cells (Fig. 6, left), H&E for general scaffold cellularity and tissue formation (Fig. 6, middle; Supporting Information Fig. S3B, S3C), and von Kossa/ van Gieson for bone formation (Fig. 6, right). All scaffolds were populated with cells and matrix as evidenced by DAPI and H&E stains. While a small amount of von Kossa staining occurred in the mCherry-transduced group with some surrounding osteoid, there was much more mineralized tissue in the PDGFB-transduced group. Of particular note, positive human-specific staining was apparent in both mCherry-transduced and PDGFB-transduced groups, indicating the human cells were still present 8 weeks postimplantation and were potentially contributing to the tissue formation within

the scaffold. As a control, the acellular scaffolds, while showing DAPI staining, had no human-specific staining, indicating the resident cells were of murine origin.

DISCUSSION

In this study, MSCs and ASCs were compared directly in their osteogenic responses to PDGF-BB. The findings reported in this study simultaneously confirm previous research showing that PDGF-BB is not directly osteoinductive on MSCs [13–17] while also confirming our more recent findings that PDGF-BB can directly enhance ASC osteogenesis [18, 27]. Both correlative (Fig. 1) and loss-of-function (Fig. 3) evidence support the observations that the divergent mineralization responses to PDGF-BB are marked. Since we have shown previously [18] that dexamethasone is not essential for mineralization of ASCs, we omitted it from this study; however, due to the prevalence of dexamethasone in MSC osteogenic culture, we also compared the mineralization response of MSCs and ASCs to PDGF-BB in the presence of 100 nM dexamethasone. While the addition of dexamethasone resulted in a twofold increase of calcium per cell for MSCs and threefold increase of calcium per cell for ASCs (Supporting Information Fig. S4), the mineralization of MSCs was still unaffected by the addition of PDGF-BB, while it was enhanced in ASCs. In particular, a key finding in this study is the differential response between MSCs and ASCs when examining the gene expression of osteogenic genes Runx2, OCN, and OSN (Fig. 2), indicating that the

observed differences in mineralization arise from fundamental genetic differences in these two cell populations. Indeed, ASC expression of Runx2 and OCN was enhanced in the presence of PDGF-BB even in the absence of osteogenic factors, indicating that PDGF-BB itself is osteoinductive to ASCs but not to MSCs.

The impetus for hypothesizing a fundamental difference between MSCs and ASCs is not new and arises from subtleties observed in the literature. For example, the generally accepted surface marker profile for ASCs includes a weakly positive CD34 population [35, 36], while MSCs are traditionally reported to be negative for CD34 [3, 35], an observation supported by this study (Supporting Information Fig. S1, bottom). In addition, ASCs possess more proliferative potential than do MSCs [37]. Most importantly, there have been several studies demonstrating a difference in potency between MSCs and ASCs, with some groups suggesting an increased capacity for osteogenic differentiation of MSCs [38, 39] and a penchant for adipogenic differentiation in ASCs [39, 40]. Despite these observations, other studies have shown that by changing culture conditions (e.g., by the addition or subtraction of growth factors), differentiation potential can be modulated between the cell types [41], thus suggesting the innate biochemistries of MSCs and ASCs are different.

While differences in potency are not generally a subject of controversy, the mechanisms underlying these differences are still poorly understood. It has been shown that MSCs express a higher preponderance of genes associated with osteogenesis [38], while ASCs display higher expression of adipogenic genes [42]. The possibility of epigenetic mechanisms underlying differences in lineage-specific gene expression has been investigated, albeit not as extensively. For instance, osteo-specific genes such as osteoglycin and osteopontin have been shown to feature different levels of methylation in MSCs and ASCs [43, 44]. While delineating genetic and epigenetic mechanisms is outside the scope of this study, the finding that gene expression of Runx2, OCN, and OSN differed between MSCs and ASCs with respect to the presence of PDGF-BB may be well-supported in this context. Taken together, previous studies into MSC and ASC stem cell biology and lineage potency provide ample motivation for rigorously delineating differences in response to growth factors.

The original impetus for investigating the role of PDGF-BB specifically in bone repair arises from its native presence in the fracture site [11, 12] and the clinical observation that injection of PDGF-BB accelerates bone regeneration [22]. Given previous results with MSCs, confirmed by the results of this study, the idea that PDGF-BB in a fracture site enhances repair in an indirect fashion is well-supported. For instance, the role of PDGF-BB in recruiting vascular-stabilizing cells is well-studied: endothelial cells invading a region secrete PDGF-BB to attract pericytes that then wrap around the nascent vasculature, stabilizing the network [21, 45]. Given the observation that bone forms around a vascular template [12, 46–48], the vascular stabilization of PDGF-BB in a fracture site may be a possible mechanism for indirect enhancement of bone repair. Such indirect mechanisms would be the sole mechanisms in a TE approach using MSCs in conjunction with PDGF-BB; however, a TE approach using ASCs instead may take advantage of a second mechanism—that the PDGF-BB may directly enhance the osteogenesis of implanted ASCs while retaining its established vascular stabilizing properties. The potential for this additional mechanism underscores the importance of critically defining differences between cell populations such that a TE graft can take full advantage of both cellular and biomolecular components.

The clinical advantages of PDGF-BB itself are underscored when comparing to the current gold standard for growth factor-based bone regenerative therapies, bone morphogenic protein 2 (BMP2). BMP2 is known to be extremely osteoinductive [49, 50] and is approved for clinical use; however, achieving a clinical effect requires supraphysiological doses, on the order of milligrams [51, 52]. Such high doses result in high costs and numerous safety concerns [53]. We have shown here and previously [18] a robust enhancement of ASC mineralization in response to 20 ng/ml PDGF-BB, a concentration comparable to physiological levels within a fracture site [11, 54]. In particular, while ASCs cultured under osteogenic (−) conditions tended to produce less calcium per cell than did identically cultured MSCs, ASCs cultured under osteogenic (+) conditions not only produced more calcium per cell than did ASCs cultured under osteogenic (−) conditions, but also produced calcium levels at or above levels from MSCs cultured under osteogenic (−) conditions (Figs. 1, 3, bottom). This observation held across the six donors investigated in this study, indicating a donor-independent phenomenon. Taken together, these considerations suggest that the use of PDGF-BB in clinical bone regenerative therapy in conjunction with ASCs may be an attractive option alongside more traditional approaches.

To illustrate the in vivo regenerative potential of TE constructs using both ASCs and PDGF-BB, the murine calvarial defect model showed a marked difference in implanted ASCs overexpressing PDGF-BB compared to implanted ASCs without PDGF-BB. CT quantification of newly mineralized tissue was evidently higher from ASCs with PDGF-BB (Fig. 5) and positive von Kossa staining in the PDGFB-transduced groups confirmed this observation (Fig. 6). We considered the possibility that the regenerated bone was solely due to invading murine cells; however, the presence of human-specific staining within both PDGFB-transduced and mCherry-transduced groups (Fig. 6, left), the stark contrast of mineralized volume between the two, and the presence of mineralized tissue in the PDGFB-transduced scaffold center (Figs. 5B, 6, right), suggests the implanted human cells directly contributed to increased bone regeneration. While there is previous data suggesting this [55], we have shown here that the contribution of implanted ASCs is greatly enhanced by the presence of PDGF-BB signaling. A more rigorous investigation on the exact contribution of implanted ASCs within an in vivo bone defect will be the subject of a future study.

CONCLUSIONS

Although MSCs can respond to PDGF-BB in a mitogenic manner, PDGF-BB does not directly induce mineralization of MSCs. In contrast, PDGF-BB directly enhances mineralization of ASCs. This difference suggests an increased efficacy for using ASCs in conjunction with PDGF-BB in TE-based approaches for bone repair and underscores the importance in delineating

differences between stem cell types in their response to biomolecules.

AUTHOR CONTRIBUTIONS

B.P.H. and D.L.H.: conception and design, collection and/or assembly of data, data analysis and interpretation, manuscript writing, and final approval of manuscript; K.L.K., C.J.B., and B.N.: collection and/or assembly of data, data analysis and interpretation, manuscript writing, and final approval of manuscript; J.J.G., A.I.C., J.M.G., A.H.D., and W.L.G.: conception and design, administrative support, data analysis and interpretation, and final approval of manuscript.

DISCLOSURE OF POTENTIAL CONFLICTS OF INTEREST

JMG is the cofounder, co-owner, and Chief Scientific Officer of LaCell LLC, a biotechnology company focusing on the clinical translation of stromal/stem cell science.

REFERENCES

1 Desai BM. Osteobiologics. Am J Orthop 2007;36:8–11.

2 Langer R, Vacanti JP. Tissue engineering. Science 1993;260:920–926.

3 Pittenger MF, Mackay AM, Beck SC et al. Multilineage potential of adult human mesenchymal stem cells. Science 1999;284:143–147.

4 Uccelli A, Moretta L, Pistoia V. Mesenchymal stem cells in health and disease. Nat Rev 2008;8:726–736.

5 Gangji V, Hauzeur JP, Matos C et al. Treatment of osteonecrosis of the femoral head with implantation of autologous bone-marrow cells. A pilot study. J Bone Joint Surg Am 2004;86-A:1153–1160.

6 Liebergall M, Schroeder J, Mosheiff R et al. Stem cell-based therapy for prevention of delayed fracture union: A randomized and prospective preliminary study. Mol Ther 2013;21:1631–1638.

7 Hart R, Komzak M, Okal F et al. Allograft alone versus allograft with bone marrow concentrate for the healing of the instrumented posterolateral lumbar fusion. Spine J 2014;14:1318–1324.

8 Fraser JK, Wulur I, Alfonso Z et al. Fat tissue: An underappreciated source of stem cells for biotechnology. Trends Biotechnol 2006;24:150–154.

9 Gimble JM, Katz AJ, Bunnell BA. Adipose-derived stem cells for regenerative medicine. Circ Res 2007;100:1249–1260.

10 Strioga M, Viswanathan S, Darinskas A et al. Same or not the same? Comparison of adipose tissue-derived versus bone marrow-derived mesenchymal stem and stromal cells. Stem Cells Dev 2012;21:2724–2752.

11 Pountos I, Georgouli T, Henshaw K et al. Release of growth factors and the effect of age, sex, and severity of injury after long bone fracture. A preliminary report. Acta Orthopaedica 2013;84:65–70.

12 Caplan AI, Correa D. PDGF in bone formation and regeneration: New insights into a novel mechanism involving MSCs. J Orthop Res 2011;29:1795–1803.

13 Yu X, Hsieh SC, Bao W et al. Temporal expression of PDGF receptors and PDGF regulatory effects on osteoblastic cells in mineralizing cultures. Am J Physiol 1997;272:C1709–1716.

14 Park SY, Kim KH, Shin SY et al. Dual delivery of rhPDGF-BB and bone marrow mesenchymal stromal cells expressing the BMP2 gene enhance bone formation in a critical-sized defect model. Tissue Eng 2013;19:2495–2505.

15 Kratchmarova I, Blagoev B, Haack-Sorensen M et al. Mechanism of divergent growth factor effects in mesenchymal stem cell differentiation. Science 2005;308:1472–1477.

16 Gruber R, Karreth F, Kandler B et al. Platelet-released supernatants increase migration and proliferation, and decrease osteogenic differentiation of bone marrow-derived mesenchymal progenitor cells under in vitro conditions. Platelets 2004;15:29–35.

17 Tokunaga A, Oya T, Ishii Y et al. PDGF receptor beta is a potent regulator of mesenchymal stromal cell function. J Bone Miner Res 2008;23:1519–1528.

18 Hutton DL, Moore EM, Gimble JM et al. Platelet-derived growth factor and spatiotemporal cues induce development of vascularized bone tissue by adipose-derived stem cells. Tissue Eng 2013;19:2076–2086.

19 Vila OF, Martino MM, Nebuloni L et al. Bioluminescent and micro-computed tomography imaging of bone repair induced by fibrin-binding growth factors. Acta Biomater 2014;10:4377–4389.

20 Hollinger JO, Hart CE, Hirsch SN et al. Recombinant human platelet-derived growth factor: Biology and clinical applications. J Bone Joint Surg Am 2008;90(Suppl 1):48–54.

21 Gehmert S, Hidayat M, Sultan M et al. Angiogenesis: The role of PDGF-BB on adipose-tissue derived stem cells (ASCs). Clin Hemorheol Microcirc 2011;48:5–13.

22 Graham S, Leonidou A, Lester M et al. Investigating the role of PDGF as a potential drug therapy in bone formation and fracture healing. Expert Opin Investig Drugs 2009;18:1633–1654.

23 Jaiswal N, Haynesworth SE, Caplan AI et al. Osteogenic differentiation of purified, culture-expanded human mesenchymal stem cells in vitro. J Cell Biochem 1997;64:295–312.

24 Worster AA, Nixon AJ, Brower-Toland BD et al. Effect of transforming growth factor beta1 on chondrogenic differentiation of cultured equine mesenchymal stem cells. Am J Vet Res 2000;61:1003–1010.

25 Hung BP, Babalola OM, Bonassar LJ. Quantitative characterization of mesenchymal stem cell adhesion to the articular cartilage surface. J Biomed Mater Res 2013;101:3592–3598.

26 Estes BT, Diekman BO, Gimble JM et al. Isolation of adipose-derived stem cells and their induction to a chondrogenic phenotype. Nat Protoc 2010;5:1294–1311.

27 Hutton DL, Kondragunta R, Moore EM et al. Tumor necrosis factor improves vascularization in osteogenic grafts engineered with human adipose-derived stem/stromal cells. PLoS One 2014;9:e107199.

28 Kozielski KL, Tzeng SY, Green JJ. A bioreducible linear poly(beta-amino ester) for siRNA delivery. Chem Commun 2013;49:5319–5321.

29 Kozielski KL, Tzeng SY, De Mendoza BAH et al. Bioreducible cationic polymer-based nanoparticles for efficient and environmentally triggered cytoplasmic siRNA delivery to primary human brain cancer cells. ACS Nano 2014;8:3232–3241.

30 Tzeng SY, Hung BP, Grayson WL et al. Cystamine-terminated poly(beta-amino ester)s for siRNA delivery to human mesenchymal stem cells and enhancement of osteogenic differentiation. Biomaterials 2012;33:8142–8151.

31 Yang X, Boehm JS, Salehi-Ashtiani K et al. A public genome-scale lentiviral expression library of human ORFs. Nat Methods 2011;8:659–661.

32 Temple JP, Hutton DL, Hung BP et al. Engineering anatomically shaped vascularized bone grafts with hASCs and 3D-printed PCL scaffolds. J Biomed Mater Res 2014;102:4317–4325.

33 Cowan CM, Shi YY, Aalami OO et al. Adipose-derived adult stromal cells heal critical-size mouse calvarial defects. Nat Biotechnol 2004;22:560–567.

34 Gupta DM, Kwan MD, Slater BJ et al. Applications of an athymic nude mouse model of nonhealing critical-sized calvarial defects. J Craniofac Surg 2008;19:192–197.

35 Mosna F, Sensebe L, Krampera M. Human bone marrow and adipose tissue mesenchymal stem cells: A user's guide. Stem Cells Dev 2010;19:1449–1470.

36 Gronthos S, Franklin DM, Leddy HA et al. Surface protein characterization of human adipose tissue-derived stromal cells. J Cell Physiol 2001;189:54–63.

37 Kern S, Eichler H, Stoeve J et al. Comparative analysis of mesenchymal stem cells from bone marrow, umbilical cord blood, or adipose tissue. Stem Cells 2006;24:1294–1301.

38 Noel D, Caton D, Roche S et al. Cell specific differences between human adipose-derived and mesenchymal-stromal cells despite similar differentiation potentials. Exp Cell Res 2008;314:1575–1584.

39 Sakaguchi Y, Sekiya I, Yagishita K et al. Comparison of human stem cells derived from various mesenchymal tissues—Superiority of synovium as a cell source. Arthritis Rheum 2005;52:2521–2529.

40 Pachon-Pena G, Yu G, Tucker A et al. Stromal stem cells from adipose tissue and bone marrow of age-matched female donors display distinct immunophenotypic profiles. J Cell Physiol 2011;226:843–851.

41 Kim HJ, Im GI. Chondrogenic differentiation of adipose tissue-derived mesenchymal stem cells: Greater doses of growth factor are necessary. J Orthop Res 2009;27:612–619.

42 Liu TM, Martina M, Hutmacher DW et al. Identification of common pathways mediating differentiation of bone marrow- and adipose tissue-derived human mesenchymal stem cells into three mesenchymal lineages. Stem Cells 2007;25:750–760.

43 Boquest AC, Noer A, Collas P. Epigenetic programming of mesenchymal stem cells from human adipose tissue. Stem Cell Rev 2006;2:319–329.

44 Arnsdorf EJ, Tummala P, Castillo AB et al. The epigenetic mechanism of mechanically induced osteogenic differentiation. J Biomech 2010;43:2881–2886.

45 Lindahl P, Hellstrom M, Kalen M et al. Endothelial-perivascular cell signaling in vascular development: Lessons from knockout mice. Curr Opin Lipidol 1998;9:407–411.

46 Maes C, Kobayashi T, Selig MK et al. Osteoblast precursors, but not mature osteoblasts, move into developing and fractured bones along with invading blood vessels. Dev Cell 2010;19:329–344.

47 Mikos AG, Herring SW, Ochareon P et al. Engineering complex tissues. Tissue Eng 2006;12:3307–3339.

48 Carano RAD, Filvaroff EH. Angiogenesis and bone repair. Drug Discovery Today 2003; 8:980–989.

49 Zegzula HD, Buck DC, Brekke J et al. Bone formation with use of rhBMP-2— (recombinant human bone morphogenetic protein-2). J Bone Joint Surg Am 1997;79A: 1778–1790.

50 Boden SD, Zdeblick TA, Sandhu HS et al. The use of rhBMP-2 in interbody fusion cages. Definitive evidence of osteoinduction in humans: A preliminary report. Spine 2000; 25:376–381.

51 Triplett RG, Nevins M, Marx RE et al. Pivotal, randomized, parallel evaluation of recombinant human Bone Morphogenetic Protein-2/absorbable collagen sponge and autogenous bone graft for maxillary sinus floor augmentation. J Oral Maxillofac Surg 2009;67:1947–1960.

52 Howell TH, Fiorellini J, Jones A et al. A feasibility study evaluating rhBMP-2 absorbable collagen sponge device for local alveolar ridge preservation or augmentation. Int J Periodontics Restorative Dent 1997;17:125–139.

53 Carragee EJ, Hurwitz EL, Weiner BK. A critical review of recombinant human bone morphogenetic protein-2 trials in spinal surgery: Emerging safety concerns and lessons learned. Spine J 2011;11:471–491.

54 Giannoudis PV, Pountos I, Morley J et al. Growth factor release following femoral nailing. Bone 2008;42:751–757.

55 Allay JA, Dennis JE, Haynesworth SE et al. LacZ and interleukin-3 expression in vivo after retroviral transduction of marrow-derived human osteogenic mesenchymal progenitors. Hum Gene Ther 1997;8:1417–1427.

See www.StemCells.com for supporting information available online.